General

Bimetallic PdCu nanoparticle decorated three-dimensional graphene hydrogel for non-enzymatic amperometric glucose sensor

Ming Yuan [a], Aiping Liu [a,b,*], Ming Zhao [a], Wenjun Dong [a], Tingyu Zhao [a], Jiajun Wang [a], Weihua Tang [c]

[a] Center for Optoelectronics Materials and Devices, Key Laboratory of Advanced Textile Materials and Manufacturing Technology, Ministry of Education, Zhejiang Sci-Tech University, Hangzhou 310018, China
[b] Key Laboratory of E&M (Zhejiang University of Technology), Ministry of Education & Zhejiang Province, Hangzhou 310032, China
[c] State Key Laboratory of Information Photonics and Optical Communication, Beijing University Posts and Telecommunications, Beijing 100876, China

ARTICLE INFO

ABSTRACT

A bimetallic PdCu nanoparticle (NP) decorated three-dimensional graphene hydrogel (PdCu/GE) was developed by a simple one-step hydrothermal method. The PdCu/GE hybrids exhibited an interconnected microporous framework with PdCu NPs dispersed and encapsulated within the GE layers. The PdCu/GE hybrids showed significant electrocatalytic activity toward glucose oxidation due to the synergistic effect of PdCu NPs and GE sheets in the alkaline solution containing chloride ions, presenting a substantial increase in the oxidation current and decrease in the onset potential of oxidation compared to the monometallic modified GE hybrids. At an applied potential of −0.4 V, the PdCu/GE modified electrode with optimized bimetallic ratio presented quick respond to glucose oxidation with a wide linear range up to 18 mM and a reproducible sensitivity of 48 $\mu A\,(mg\,mM)^{-1}$ in the presence of chloride ions. Furthermore, the PdCu/GE modified electrode exhibited high selectivity to glucose and resistance against poisoning by commonly interfering species such as dopamine, ascorbic acid, uric acid, acetamidophenol and some monosaccharides. The PdCu/GE hybrid hydrogels with 3D micropores were therefore promising for the future development of non-enzymatic amperometric glucose sensors with improved electrochemical performances.

© 2013 Elsevier B.V. All rights reserved.

1. Introduction

Since diabetes is characterized by an abnormal level of blood glucose induced by the defects in insulin production and insulin action, the development of fast, accurate and reliable methods for glucose determination is essential in clinical diagnostics, food industry and biotechnology. Though the amperometric glucose sensors based on glucose oxidases present high sensitivity and selectivity, their application is restricted by the intrinsic nature of the enzymes including the instability, sensitive to environment factors (temperature, pH value and ionic detergents), high cost and complicated immobilization procedure [1,2]. Therefore, a simple enzyme-free glucose sensor with low cost, reproducibility, interference free and reliably fast determination seems to be an attractive technique free from above-mentioned drawbacks. Among non-enzymatic glucose sensors, the electrochemical biosensors have been considered as one of the most popular and effective

techniques for glucose detection due to their advantages in terms of simplicity, portability, short response time, high sensitivity and selectivity by substrate specificity [3]. Many noble metals [4,5], metal alloys [6–8] and metal oxide nanoparticles (NPs) and nanostructures [9,10] have been used to develop non-enzymatic amperometric electrodes due to their excellent catalytic performances. Among these, bimetallic PdCu alloys and nanocomposites have attracted considerable attention as highly active, eco-friendly and relatively cheaper catalysts for use in fuel cells [11–16] and glucose sensor [17]. Since the lattice mismatch between Pd and Cu is about 7.1%, the bimetallic alloy, bimetallic nanocrystals with core–shell structures or nanocomposites can be formed [18]. Recent study indicates that the nanotubular and nanoporous PdCu bimetallic catalysts dispersed on carbon powder have a higher catalytic activity than the conventional PdCu metal alloy for oxygen reduction reaction [11]. However, the electrochemical activity of this bimetallic catalyst for glucose oxidation is still given little attention.

Consideration for the possible dissolution, sintering and agglomeration of metal-based catalysts during operation of catalytic reaction, nanostructured carbon materials including porous carbon, active carbon, diamond-like carbon, carbon nanotubes and

* Corresponding author. Tel.: +86 571 86843468;
fax: +86 571 86843222/+86 571 86843468.
E-mail address: liuaiping1979@gmail.com (A. Liu).

graphene (GE) are usually imported as catalyst supports to provide a large electroactive surface area and improve activity and durability of catalysts. Among these, the two-dimensional GE nanosheet with carbon atoms packed in a hexagonal lattice is regarded as a new-generation catalyst support due to its excellent conductivity, high surface area, extraordinary chemical and environmental stability and strong adhesion ability for metal catalyst [19–22]. The hybridization of GE with metallic nanomaterials might yield new properties via their cooperative interaction and promote electron transfer on the metal catalyst. However, the π–π interaction of GE sheets makes the aggregation and stacking emergence, which decreases the electrolyte diffusion, compromises the specific surface area and damages the catalyst performance [23]. Recent research indicates that three-dimensional (3D) GE-based nanomaterials [23–26] might overcome this obstacle since their ideally interconnected porous structure for catalyst loading could facilitate the mass transfer and maximize the accessibility for reactants to the active catalyst surfaces [27]. This makes them promising for the future development of sensors, fuel cells, supercapacitors and lithium-ion batteries [23,26–30]. For example, Dong et al. fabricated a 3D Co_3O_4/GE electrode using a simple hydrothermal procedure combined with chemical vapor deposition and found its high electrocatalytic activity for glucose detection [23]. Hu et al. prepared ternary Pt/PdCu nanoboxes anchored on a 3D GE framework, which might be used in fuel cells, by a dual solvothermal strategy [27]. However, to the best of our knowledge, there are few reports on 3D GE encapsulated PdCu hybrids for nonenzymatic glucose detection. In this paper, we fabricated a reliable enzymatic-free glucose sensor based on the 3D PdCu/GE hydrogel modified ITO electrode by a facile one-step hydrothermal method. The PdCu/GE hybrids were characterized by X-ray diffraction (XRD), scanning electron microscopy (SEM), transmission electron microscope (TEM) and X-ray photoelectron spectrometer (XPS). The outstanding catalytic ability of the as-prepared PdCu/GE hybrid enabled it to quantitatively detect glucose in a wide range with a low detection limit without common interference from dopamine (DA), ascorbic acid (AA), uric acid (UA), acetamidophenol (AP) and monosaccharide (fructose).

2. Experimental section

2.1. Reagents

D-Glucose, $CuSO_4 \cdot 5H_2O$ and $PdCl_2$ (purity 99.99%) were supplied by Sigma, USA. Nafion in ethanol solution (5 wt%) was purchased from Sigma-Aldrich. Graphite powder was supplied by Qingdao Huatai Tech. Co. Ltd. Other reagents were commercially available and of analytical reagent grade. Deionized water with resistance of approximately 18 MΩ cm was used throughout the experiment.

2.2. Preparation of PdCu/GE hybrid hydrogels

The graphene oxide (GO) was prepared from natural graphite by using modified Hummers' method [31]. The palladium(II) and copper(II) salts with different mass ratios, glutamate, GO and ethylene glycol were mixed and the aqueous dispersion was sealed in a stainless-steel autoclave and maintained at 100 °C for 3 h to prepare the PdCu/GE hydrogels by a facile one-step hydrothermal strategy [15]. The GE, Pd/GE and Cu/GE hydrogels were fabricated with the same method. The resultant PdCu/GE composites (the inset in Fig. 1A) were labeled as Pd_xCu_y/GE according to the mass percents of Pd and Cu in the composites (*x* and *y* were the percent contents of Pd and Cu, respectively). After the hydrothermal treatment was completed, the autoclave was cooled and the as-prepared samples were washed with distilled water and freeze-dried overnight.
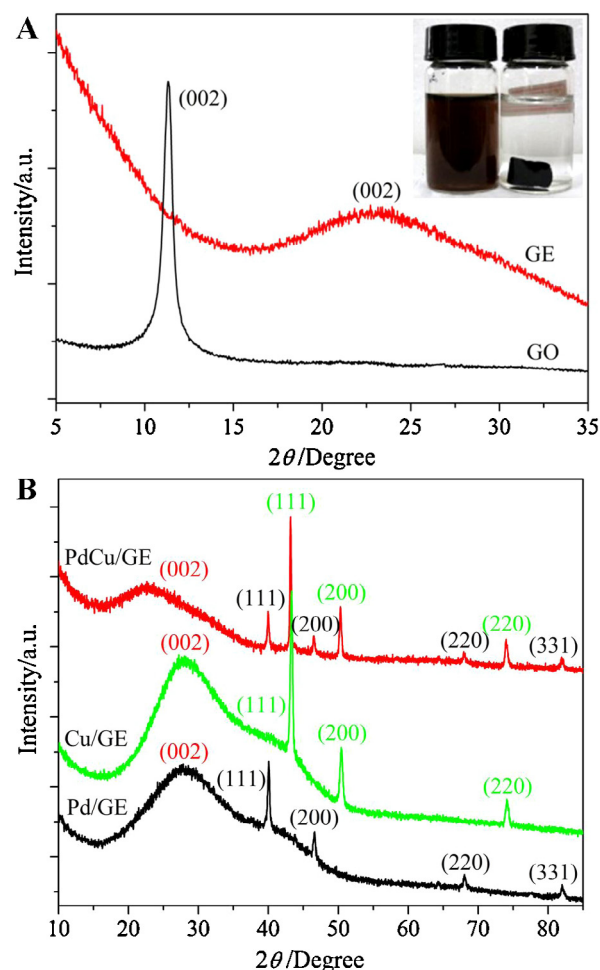

Fig. 1. X-ray diffraction patterns of (A) GO and GE and (B) Pd/GE, Cu/GE and $Pd_{66}Cu_{34}$/GE hydrogels. The inset in (A) is the photograph of the mixed solution including palladium(II) and copper(II) salts and GO before hydrothermal reaction and $Pd_{66}Cu_{34}$/GE hydrogel after hydrothermal reaction.

For electrode preparation, the ITO glasses were rinsed by ethanol and distilled water and dried in N_2. The 1 mg of catalyst powder was mixed with 1 mL of distilled water and 1 mL of Nafion in ethanol solution (0.5 wt%), and then the dispersion was ultrasonically treated to form the ink (catalyst dispersion). Approximately 40-μL ink was dropped onto the clean ITO electrode and subsequently dried under vacuum for 2 h at room temperature.

2.3. Characterization and measurements

The elemental composition and XPS core level spectra of freeze-dried hydrogels were collected by XPS (KRATOS AXIS ULTRA-DLD) with the binding energies calibrated by C 1s as reference energy (C 1s = 284.6 eV). The XRD patterns of different complex were obtained on a diffractometer (Bruker AXS D8) using the Cu Kα radiation (λ = 0.15418 nm) with the 2θ scan from 5° to 90° at a step of 0.02°. The morphologies of different hydrogels were obtained by the SEM (Hitachi S4800) and TEM (Hitachi H-7650) performed at an acceleration voltage of 200 kV.

The electrochemical measurements were carried out with a CHI660B electrochemical workstation (Shanghai Chenhua Instrument Factory, China) in a three-electrode cell, which consisted of a working electrode, a platinum counter electrode and a reference electrode (saturated calomel electrode, SCE) in the alkaline solution with nitrogen saturated. All currents obtained on the
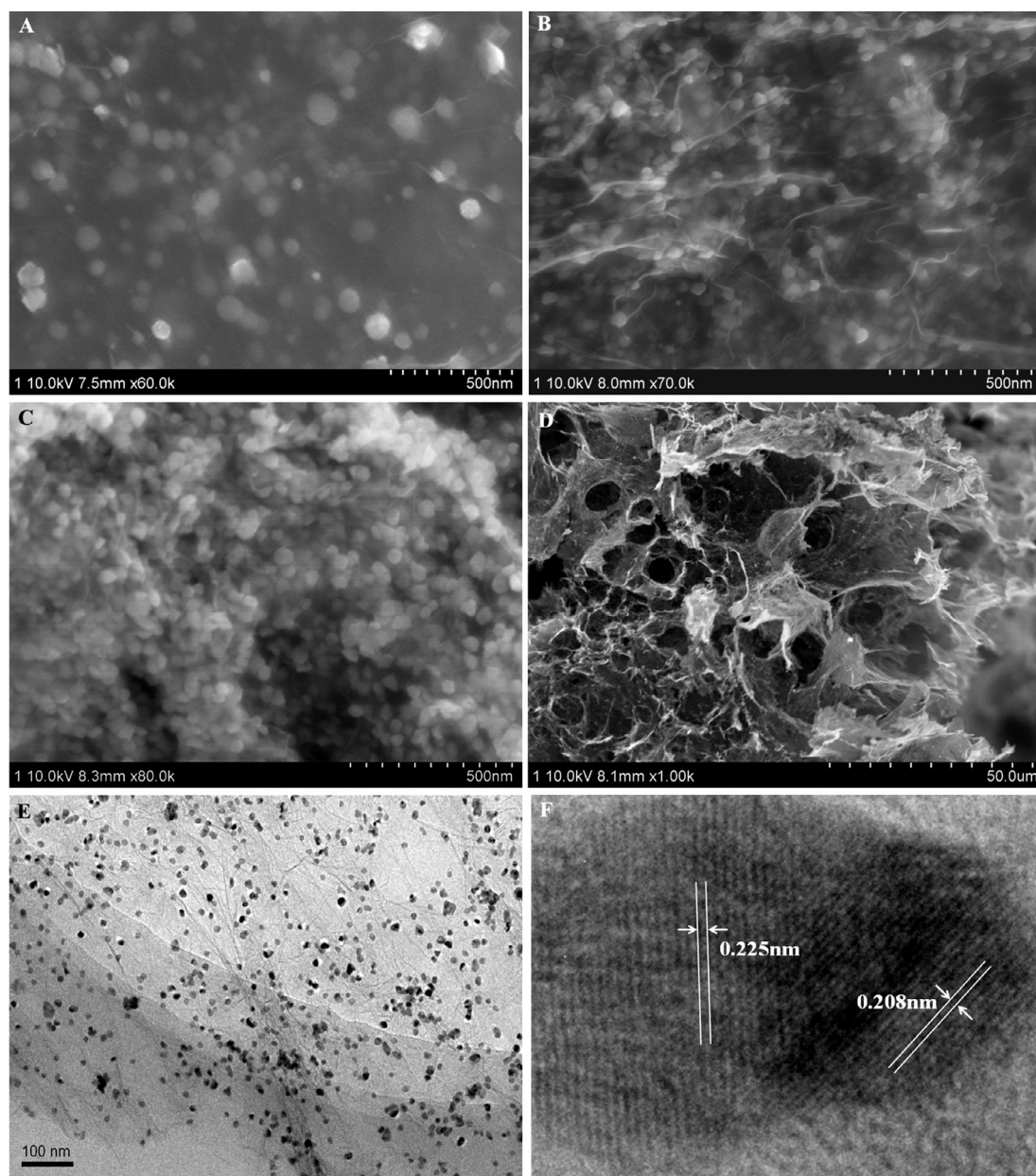
Fig. 2. Scanning electron microscopy images of (A) Cu/GE, (B) Pd/GE, (C) and (D) $Pd_{66}Cu_{34}$/GE hydrogels with different magnifications. (E) Transmission electron microscope and (F) high-resolution TEM images of PdCu NPs on GE sheet.

electrodes were normalized to the total catalyst loading on each electrode.

3. Results and discussion

### 3.1. Microstructures of PdCu/GE hydrogels

The XRD patterns of GE and different metal/GE hydrogels are displayed in Fig. 1. The diffraction peak at 11.2° for GO can be assigned to the (0 0 2) reflection of the hexagonal graphite structure. After hydrothermal reaction, this characteristic peak moves to 23.3°, indicating the successful reduction from GO to GE (Fig. 1A). The broad diffraction peaks of GE and metal/GE hydrogels at about 22°–28° might be attributed to the diffraction signals of small amounts of GE layers with poor ordering along their stacking directions [24,32]. The well-resolved peaks at 40.1°, 46.4°, 67.9° and 81.9° for Pd/GE and those at 43.3°, 50.3° and 74.2° for Cu/GE in

Fig. 1B can be indexed as the (1 1 1), (2 0 0), (2 2 0) and (3 3 1) crystalline planes of Pd (JCPDS card no. 46-1043) [33] and (1 1 1), (2 0 0) and (2 2 0) crystalline planes of Cu (JCPDS card no. 85-1326) [34]. Our results indicate that the as-synthesized PdCu/GE nanostructures are bimetallic composites rather than PdCu alloys. This might be attributed to the difference of nucleation rates of Pd and Cu on the GE surface. In the case of Pd existence, the Cu might have a tendency to nucleate and grow on one face of the Pd seed [18].

The SEM images of different hybrids are shown in Fig. 2. The hybrids exhibit an interconnected, porous 3D framework with the Cu, Pd and PdCu NPs uniformly dispersed on both sides of the GE sheets, even encapsulated within the GE layers (Fig. 2A–C). This might be attributed to the residual oxygen functionalities or oxygen defects on GE sheets which make the assembly between the NPs and the GE sheets more efficient [23,27]. The structure with metallic NPs encapsulated within GE layers is benefit for enhancing their interface contact and suppressing the dissolution and
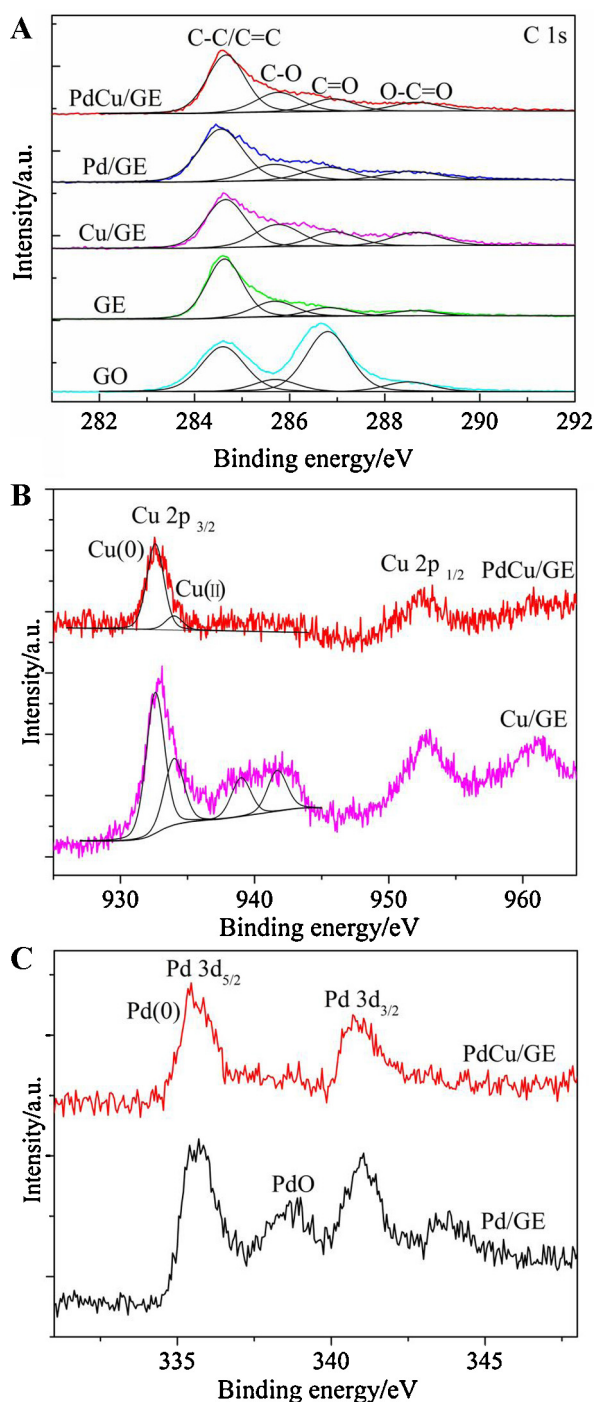
Fig. 3. Deconvoluted X-ray photoelectron spectra of GO, GE, Cu/GE, Pd/GE, and Pd$_{66}$Cu$_{34}$/GE hydrogels: (A) C 1s, (B) Cu 2p and (C) Pd 3d.

agglomeration of metallic NPs, thereby promoting the electrochemical activity and stability of the hybrids [28,35]. TEM characterization further validates the uniform distribution of PdCu NPs on flake-like wrinkled GE (Fig. 2E). The lattice fringe distances of 0.208 nm and 0.225 nm could be ascribed to the (1 1 1) lattice spacings of face-centered cubic Cu [32] and face-centered cubic Pd [36] (Fig. 2F), respectively. These are fitted well with the calculated values of 0.209 nm for Cu and 0.228 nm for Pd based on the XRD data.

Furthermore, the deconvoluted XPS spectra of different hydrogels are plotted in Fig. 3. The four peaks at 284.6 ± 0.1 eV, 285.7 ± 0.1 eV, 286.9 ± 0.1 eV and 288.6 ± 0.1 eV for C 1s spectra

are corresponding to the C–C/C=C, C–O, C=O and O–C=O bonds [22,37], respectively (Fig. 3A). The C/O atomic percentage increases from 1.73 for GO to 4.23 for GE, demonstrating the reduction from GO to GE with fewer oxygen functionalities [37]. The remarkable signal associated with oxygen for Cu/GE (C/O atomic percentage of 3.47) is due to the nature of easy oxidization in air for Cu NPs. This can be deduced from Cu 2p spectra. The peaks at 932.5 ± 0.1 eV and 952.3 ± 0.1 eV are attributed to Cu 2p$_{3/2}$ and Cu 2p$_{1/2}$, respectively (Fig. 3B). The Cu 2p$^{3/2}$ peak can be further deconvoluted into two peaks at 932.6 ± 0.1 eV and 934.0 ± 0.1 eV, which may be attributed to Cu(0) and Cu(II), respectively, suggesting the copper oxide existence on the Cu surface [38]. The peaks at 939.0 ± 0.1 eV and 941.8 ± 0.1 eV are the satellite peaks of Cu(II) [39]. The two peaks, at 335.6 ± 0.1 eV and 340.8 ± 0.1 eV can be assigned to Pd 3d$_{5/2}$ and Pd 3d$_{3/2}$ regions, respectively, indicating the existence of metallic Pd(0) [40] (Fig. 3C). Furthermore, the peaks at 338.6 ± 0.1 eV and 343.8 ± 0.1 eV show more than one chemical state of Pd in Pd/GE. By comparison, the pristine copper and palladium are predominant for the PdCu/GE hydrogel. The XPS data indicate that the PdCu/GE hydrogel with fewer oxygen functionalities presents effective reducing not only for GE but also for the decorated NPs and the bimetallic modified GE hybrid has a stronger antioxidant capacity than the monometallic modified ones.

3.2. Electrocatalytic activities of PdCu/GE hydrogels toward glucose oxidation

The electrocatalytic activities of PdCu/GE hybrids are investigated using cyclic voltammetry (CV) in a N$_2$-saturated 0.1 M NaOH solution with and without 10 mM glucose at a scan rate of 50 mV s^{-1}. As shown in Fig. 4A, neither the GE modified ITO electrode nor the Cu/GE modified one shows obvious electrocatalytic activity for glucose oxidation. The current in the potential region from −0.80 V to −0.60 V is mainly due to the adsorption/desorption of hydrogen ad-atoms and the current in the potential range from 0.20 V to 0.40 V is ascribed to the oxygen evolution on Cu/GE modified electrode. The small peak centered at about −0.50 V in the negative scan for Cu/GE hybrid corresponds to the reduction peak to Cu ions. For the Pd/GE and PdCu/GE modified ITO electrodes, the peak A in the potential region from −0.30 V to 0.15 V at the positive scan in the 0.1 M NaOH solution is related to the formation of Pd–OH$_{ads}$ and Pd oxide (PdO) (Fig. 4B) [21,41]. At the negative scan, the strong cathodic peak B centered at −0.34 V is related to the reduction of Pd oxide formed in the positive scan. With the addition of glucose, an obvious increase in current on Pd/GE surface, starting at about −0.55 V (Peak C), and an obvious oxidation peak D at around −0.1 V correspond to the oxidation of glucose at the positive scan. The Peak C could be attributed to the glucose electroadsorption, causing the generation of an adsorbed intermediate and one proton transfer [42]. When the applied potential increases over −0.30 V, the Pd–OH$_{ads}$ species are generated in the alkaline solution which favors the oxidation of adsorbed glucose to gluconolactone or gluconic acid (peak D). As the reaction continues, the accumulation of oxidation products and the aggravation of Pd oxidation on the electrode surface further inhibit the adsorption and oxidation of glucose, resulting in current decrease when the potential over 0.10 V. This suggests that the Pd–OH$_{ads}$ species play a major role in the oxidation of glucose [21,41]. During the negative scan, the oxidized Pd surfaces are reduced at a potential around −0.20 V. The glucose oxidation occurs when more surface-active sites are renewed, resulting in a large peak current in the potential range from −0.34 V to −0.65 V (peak E) [43]. In contrast, the PdCu/GE hybrids display higher electrocatalytic activities for the glucose oxidation which starts at a lower potential about −0.70 V. Larger oxidation currents are obtained on Pd$_{80}$Cu$_{20}$/GE,
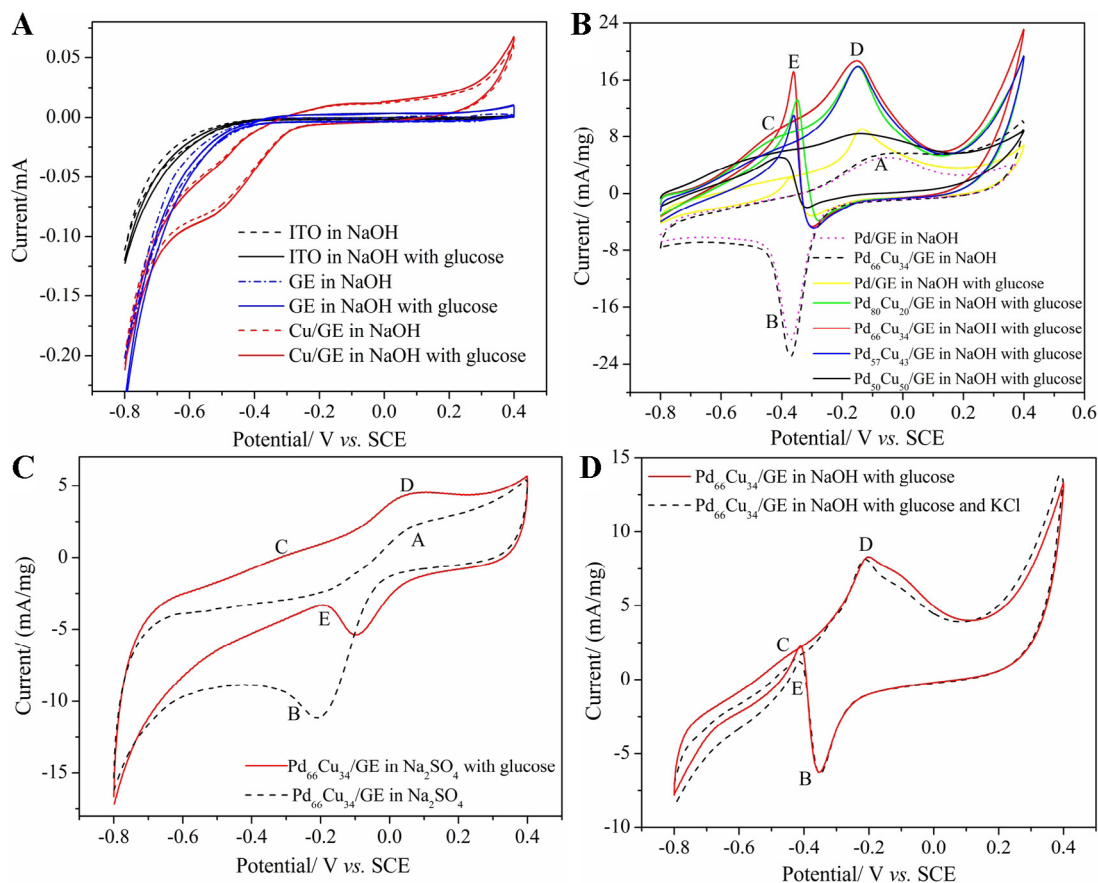
Fig. 4. Cyclic voltammograms of (A) ITO, GE modified ITO and Cu/GE modified ITO electrodes, (B) Pd/GE and PdCu/GE modified ITO electrodes in the absence and presence of 10 mM glucose in the N_2-saturated 0.1 M NaOH with the scan rate of 50 mV s^{-1}. (C) Cyclic voltammograms of $Pd_{66}Cu_{34}$/GE modified ITO electrodes in the absence and presence of 10 mM glucose in the N_2-saturated 0.1 M Na_2SO_4 with the scan rate of 50 mV s^{-1}. (D) Cyclic voltammograms of $Pd_{66}Cu_{34}$/GE modified ITO electrodes in the N_2-saturated 0.1 M NaOH and 5 mM glucose solution with and without 0.15 M KCl at the scan rate of 50 mV s^{-1}.

$Pd_{66}Cu_{34}$/GE and $Pd_{57}Cu_{43}$/GE modified electrodes. With the copper proportion further increase, the $Pd_{50}Cu_{50}$/GE hybrid presents a lower starting point for glucose oxidation at about -0.75 V concomitant the decrease of current signal. This indicates the cooperative effect of Pd and Cu NPs. The Pd sites in the complex, with lower electron occupancy in their 3d orbitals in comparison to the Cu sites, could function as Lewis acid sites for adsorption of polar glucose molecules, which are Lewis bases, via their non-bonded electron pairs [17,44]. An optimal component is therefore beneficial for the electrocatalytic activity improvement, cost decrease and long-term stability of hybrids. Further, the 3D GE with adequate oxygen functionalities could effectively favor the nucleation of metallic NPs, the accessibility for reactants to the active catalyst surfaces and the enhancement of reaction dynamics [23,37]. Therefore, the bimetallic NPs and interconnected porous GE framework play a synergistic effect in the performance improvement of complex. Furthermore, the CV response of glucose oxidation on the PdCu/GE modified electrode is also detected in the neutral environment (0.1 M Na_2SO_4 solution). Different from Pt-based catalysts, which have excellent catalytic activity for glucose oxidation in the neutral PBS solution (pH 7.0–7.4) [45–49], the oxidation current signal of glucose obtained on the present PdCu/GE catalyst is significant weakened in the neutral environment compared to that obtained in the alkaline media (Fig. 4C). In fact, many Pd-based catalysts display favorable catalytic ability for glucose oxidation in the alkaline environment [17,21]. This might be attributed to the more Pd–OH$_{ads}$ species formed on the PdCu/GE surface in a lower potential in the alkaline environment (Fig. 4B and C). Therefore, the electrochemical measurement in the present paper is carried out in

the alkaline environment. Consideration the possible impairation of chloride ions on the Pd-based catalysts, we study the poisoning resistance of the PdCu/GE modified electrode upon chloride ions. Only 5–10% reduce in current can be detected when the 0.15 M KCl solution is added in the NaOH solution (Fig. 4D), indicating the good poisoning resistance of the PdCu/GE hybrid to the environment containing Cl$^-$.

Since the good performance of $Pd_{66}Cu_{34}$/GE modified electrode for glucose oxidation, the electrode is further used to detect the glucose with different concentrations. Fig. 5A shows the CV curves of oxidation current signal upon the addition of glucose. The anodic peak current of glucose oxidation increases with increasing glucose concentration concomitant the peak potential shifting to a more positive region (from -0.2 V to -0.1 V for peak D). The peak current vs. glucose concentration plot (Fig. 5B) is highly linear ($R = 0.998$) in the range of 2–18 mM (covering blood glucose levels in diabetic patients), pointing to the potential of $Pd_{66}Cu_{34}$/GE modified electrode for developing a generic non-enzymatic glucose sensor. The relative standard deviation (RSD) of 4–4.8% is calculated based on six CV measurements at the as-prepared $Pd_{66}Cu_{34}$/GE modified electrodes with successive glucose addition, revealing an excellent repeatability of the electrodes. The current-time response of $Pd_{66}Cu_{34}$/GE modified electrode to glucose oxidation at a potential of -0.4 V is also studied in the N_2-saturated 0.1 M NaOH containing 0.15 M KCl with a step of 1 mM glucose added to evaluate the performance of glucose sensor. It can be seen from Fig. 6A that the current response increases immediately and reaches 95% of the steady state value within 5–10 s with the successive additions of glucose. The current response of the sensor exhibits a linear

Table 1
Parameter comparison of different glucose sensors.

Electrode material	Detection potential (V)	Linear range (mM)	Detection limit (μM)	Sensitivity (μA cm^{-2} mM^{-1})	Reference
PdCu/GE	−0.4	1–18	20	48 (μA mg^{-1} mM^{-1})	This work
Pt–Au alloy	+0.3	0–11	6	352	[45]
PtNi/GE	−0.35	0.5–35	10	20.42	[47]
PtCu nanochains	−0.1	0.01–17	2.5	135	[48]
Pt–Pd nanoflakes	−0.3	0–16	20.6	48	[49]
Pd/GE	+0.4	0.01–5	1	N.A.	[21]
Pd-doped copper oxide nanofibers	+0.32	0.2×10^{-3}–2.5	190	1061.4	[17]
Pd/CNT	−0.35	0.5–17	0.2	160	[50]
PtCu alloys with glucose oxidase	+0.8	0.6–15	100	N.A.	[51]
PdCu alloy with glucose oxidase	+0.8	0.5–20	1	N.A.	[52]
Cu/Pd Coating with glucose oxidase	+0.70	up to 6.0	0.1	7.3 (μA mM^{-1})	[53]

dependence on glucose concentration ($R = 0.998$) in the range from 1 mM to 18 mM with the sensitivity of 48 μA (mg mM)$^{-1}$ and a detection limit of 20 μM (signal/noise = 3) (Fig. 6B). The RSD up to 5.0% is calculated based on six measurements at the as-prepared Pd$_{66}$Cu$_{34}$/GE modified electrode with successive glucose addition. The performance of our sensor is comparable if not superior to those reported on other literatures listed in Table 1. Therefore, the PdCu/GE modified electrode is promising for the determination of blood sugar concentration in the practical clinical analysis when considering its easy fabrication, quick response, wide detection range and non-enzymatic detection at a negative potential (−0.4 V). Our further work will be carried out to improve the performance of PdCu/GE catalyst in the neutral solution by varying the proportions of the GO and two metallic precursors.

3.3. Interference, repeatability and real sample analysis

We further investigate the amperometric response of Pd$_{66}$Cu$_{34}$/GE modified ITO electrode for the reference substances including DA, AA, UA, AP and monosaccharide (fructose) which normally coexist with glucose in the human blood. The amperometric response of the Pd$_{66}$Cu$_{34}$/GE modified ITO electrode toward 1 mM glucose, 1 mM DA, 1 mM AA, 1 mM UA, 1 mM AP and 1 mM fructose in the N$_2$-saturated 0.1 M NaOH containing 0.15 M KCl is shown in Fig. 7. The current responses produced by DA, AA, UA, AP and fructose are only 10–16% of that of glucose (set to 1).
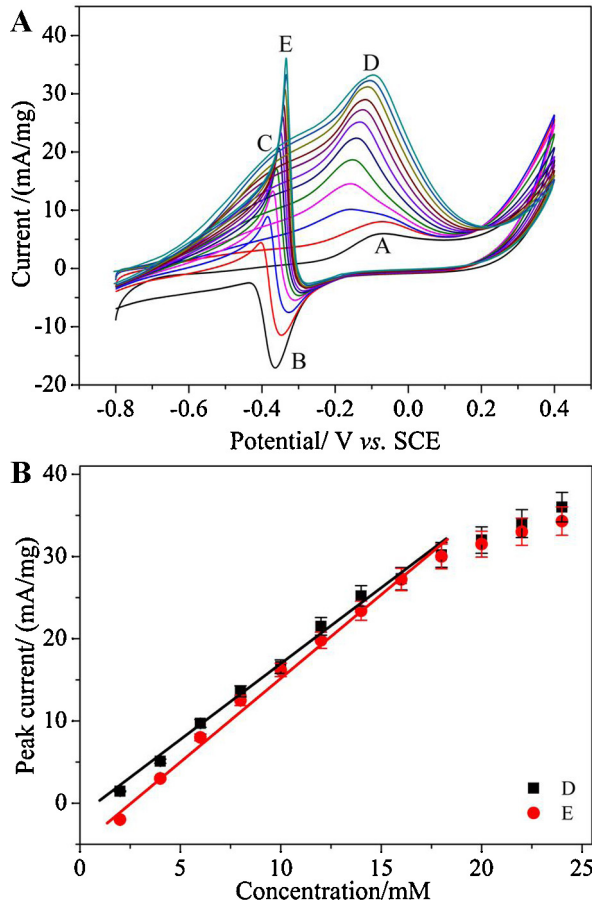

Fig. 5. (A) Cyclic voltammograms of Pd$_{66}$Cu$_{34}$/GE modified ITO electrode in the N$_2$-saturated 0.1 M NaOH with different concentrations of glucose at the scan rate of 50 mV s^{-1}. (B) Linear relations of peak currents of D and E with glucose concentration. Error bars indicate the relative standard deviations of six measurements. The straight line indicates the calibration curve.
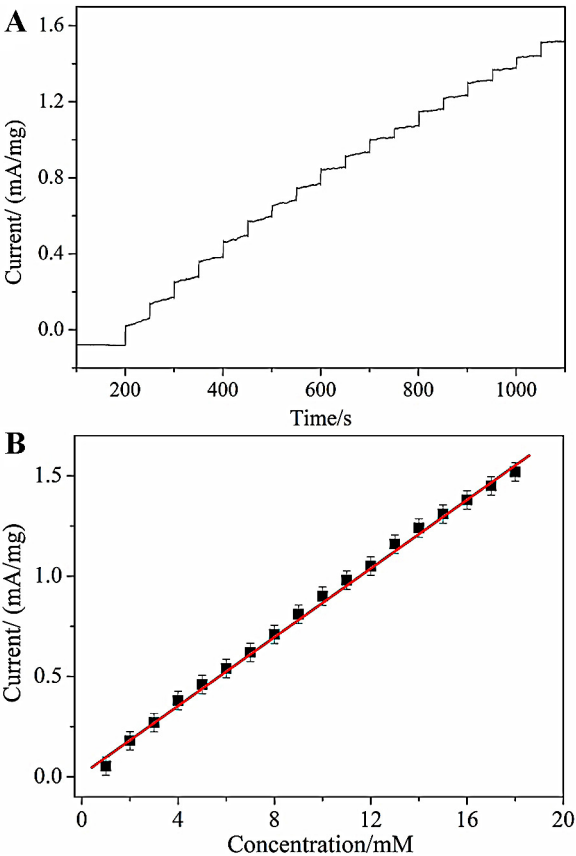
Fig. 6. (A) Typical current–time curve of glucose oxidation at the Pd$_{66}$Cu$_{34}$/GE modified ITO electrode with the successful addition of glucose from 1 mM to 18 mM into the N$_2$-saturated 0.1 M NaOH solution containing 0.15 M KCl at −0.4 V. (B) Linear relation of current response with glucose concentration. Error bars indicate the relative standard deviations of six measurements. The red line indicates the calibration curve.
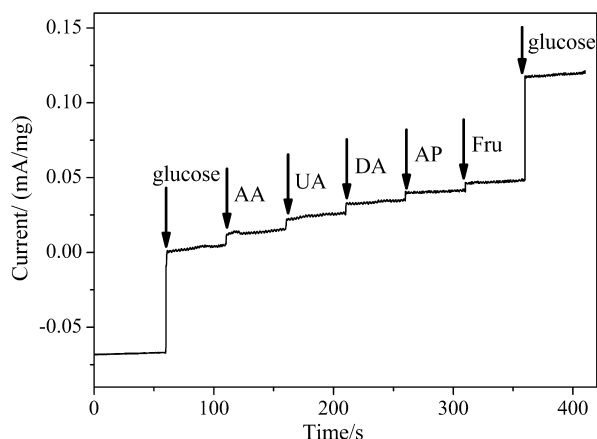
Fig. 7. Interference test of the $Pd_{66}Cu_{34}$/GE modified ITO electrode in N_2-saturated 0.1 M NaOH containing 0.15 M KCl solution with 1 mM glucose, 1 mM dopamine (DA), 1 mM ascorbic acid (AA), 1 mM uric acid (UA), 1 mM acetamidophenol (AP) and 1 mM fructose (Fru) at −0.40 V.

The addition of interfering species does not significantly decline the sensor response for the second added glucose. The Nafion in the modified electrode is helpful to provide a repelling effect toward the negative changed AA, UA and AP, resulting in high selectivity to glucose.

The reproducibility and repeatability of the developed sensor is determined and the RSD of amperometric current responses recorded by 20 injections of 1 mM glucose in the 0.1 M NaOH solutions is calculated to be about 5.0%. The stability of the developed sensor is investigated over a 60-day period. The oxidation current of glucose exhibits a sharp drop to about 80% of the initial response after 2 weeks due to the absence of some PdCu NPs. However, the current response remains relatively stable throughout the rest of the 60-day period, implying a long-term stability of the sensor.

The analysis capability of the developed sensor for the real sample is investigated by adding 40.0 μL of human serum sample in the 10.0 mL of 0.1 M NaOH solution. The current response for glucose at −0.40 V is determined by the RSD of pure glucose to the solutions containing the serum samples, and the relative standard deviation recorded by the injections of 0.5 mM glucose in five solutions is calculated to be about 4.5%, indicating the good stability and reproducibility of the electrode in real serum sample.

4. Conclusion

We developed a 3D microporous PdCu/graphene (PdCu/GE) hydrogel by a one-step hydrothermal method. The bimetallic PdCu catalysts were excellently dispersed and encapsulated on the 3D framework of GE sheets with high surface area and adequate oxygen functionalities. The optimal PdCu/GE modified electrode presented high electrocatalytic activities toward glucose oxidation due to a synergistic effect from bimetallic nanoparticles and porous GE, which was beneficial for the electrocatalytic activity improvement, cost decrease and long-term stability of hybrids. The PdCu/GE modified electrode displayed a broad detection range up to 18 mM (covering blood glucose levels in diabetic patients) with the detection limit about 20 μM for glucose oxidation in the alkaline solution containing chloride ions. The easy fabrication procedure, fast response, high catalytic activity and good specificity in the presence of common interferents such as dopamine, ascorbic acid, uric acid, acetamidophenol and some monosaccharides favor the PdCu/GE hydrogel potential application as non-enzymatic amperometric glucose sensors.

References

[1] R. Wilson, A.P.F. Turner, Glucose-oxidase: an ideal enzyme, Biosens. Bioelectron. 7 (1992) 165–185.
[2] I. Katakis, E. Dominguez, Characterization and stabilization of enzyme biosensors, TrAC—Trends Anal. Chem. 14 (1995) 310–319.
[3] J. Wang, Electrochemical glucose biosensors, Chem. Rev. 108 (2008) 814–825.
[4] A.P. Liu, Q.H. Ren, T. Xu, M. Yuan, W.H. Tang, Morphology-controllable gold nanostructures on phosphorus doped diamond-like carbon surfaces and their electrocatalysis for glucose oxidation, Sens. Actuators, B—Chem. 162 (2012) 135–142.
[5] J.H. Yuan, K. Wang, X.H. Xia, Highly ordered platinum-nanotubule arrays for amperometric glucose sensing, Adv. Func. Mater. 15 (2005) 803–809.
[6] X.L. Chen, H.B. Pan, H.F. Liu, M. Du, Nonenzymatic glucose sensor based on flower-shaped Au@Pd core–shell nanoparticles–ionic liquids composite film modified glassy carbon electrodes, Electrochim. Acta 56 (2010) 636–643.
[7] F.J. Miao, B.R. Tao, L. Sun, T. Liu, J.C. You, L.W. Wang, et al., Amperometric glucose sensor based on 3D ordered nickel–palladium nanomaterial supported by silicon MCP array, Sens. Actuator, B—Chem. 141 (2009) 338–342.
[8] C.Z. Zhu, S.J. Guo, S.J. Dong, PdM (M = Pt, Au) bimetallic alloy nanowires with enhanced electrocatalytic activity for electro-oxidation of small molecules, Adv. Mater. 24 (2012) 2326–2331.
[9] H. Wei, E.K. Wang, Fe_3O_4 magnetic nanoparticles as peroxidase mimetics and their applications in H_2O_2 and glucose detection, Anal. Chem. 80 (2008) 2250–2254.
[10] W. Wang, L.L. Zhang, S.F. Tong, X. Li, W.B. Song, Three-dimensional network films of electrospun copper oxide nanofibers for glucose determination, Biosens. Bioelectron. 25 (2009) 708–714.
[11] L. Xiong, Y.X. Huang, X.W. Liu, G.P. Sheng, W.W. Li, H.Q. Yu, Three-dimensional bimetallic Pd–Cu nanodendrites with superior electrochemical performance for oxygen reduction reaction, Electrochim. Acta 89 (2013) 24–28.
[12] C.X. Xu, A.H. Liu, H.J. Qiu, Y.Q. Liu, Nanoporous PdCu alloy with enhanced electrocatalytic performance, Electrochem. Commun. 13 (2011) 766–769.
[13] C.G. Hu, Y.M. Guo, J.L. Wang, L. Yang, Z.X. Yang, Z.Y. Bai, et al., Additive-free fabrication of spherical hollow palladium/copper alloyed nanostructures for fuel cell application, ACS Appl. Mater. Interfaces 4 (2012) 4461–4464.
[14] N.N. Kariuki, X.P. Wang, J.R. Mawdsley, M.S. Ferrandon, S.G. Niyogi, J.T. Vaughey, et al., Colloidal synthesis and characterization of carbon-supported Pd–Cu nanoparticle oxygen reduction electrocatalysts, Chem. Mater. 22 (2010) 4144–4152.
[15] L. Yang, C.G. Hu, J.L. Wang, Z.X. Yang, Y.M. Guo, Z.Y. Bai, et al., Facile synthesis of hollow palladium/copper alloyed nanocubes for formic acid oxidation, Chem. Commun. 47 (2011) 8581–8583.
[16] W.D. Kang, Y.C. Wei, C.W. Liu, K.W. Wang, Enhancement of electrochemical properties on Pd–Cu/C electrocatalysts toward ethanol oxidation by atmosphere induced surface and structural alteration, Electrochem. Commun. 13 (2011) 162–165.
[17] W. Wang, Z.Y. Li, W. Zheng, J. Yang, H.N. Zhang, C. Wang, Electrospun palladium(IV)-doped copper oxide composite nanofibers for non-enzymatic glucose sensors, Electrochem. Commun. 11 (2009) 1811–1814.
[18] M.S. Jin, H. Zhang, J.G. Wang, X.L. Zhong, N. Lu, Z.Y. Li, et al., Copper can still be epitaxially deposited on palladium nanocrystals to generate core–shell nanocubes despite their large lattice mismatch, ACS Nano 6 (2012) 2566–2573.
[19] Y.Y. Shao, J. Wang, H. Wu, J. Liu, I.A. Aksay, Y.H. Lin, Graphene based electrochemical sensors and biosensors: a review, Electroanalysis 22 (2010) 1027–1036.
[20] T. Kuila, S. Bose, P. Khanra, A.K. Mishra, N.H. Kim, J.H. Lee, Recent advances in graphene-based biosensors, Biosens. Bioelectron. 26 (2011) 4637–4648.
[21] L.M. Lu, H.B. Li, F.L. Qu, X.B. Zhang, G.L. Shen, R.Q. Yu, In situ synthesis of palladium nanoparticle–graphene nanohybrids and their application in nonenzymatic glucose biosensors, Biosens. Bioelectron. 26 (2011) 3500–3504.
[22] C.S. Shan, H.F. Yang, J.F. Song, D.X. Han, A. Ivaska, L. Niu, Direct electrochemistry of glucose oxidase and biosensing for glucose based on graphene, Anal. Chem. 81 (2009) 2378–2382.
[23] X.C. Dong, H. Xu, X.W. Wang, Y.X. Huang, M.B. Chan-Park, H. Zhang, et al., 3D graphene–cobalt oxide electrode for high-performance supercapacitor and enzymeless glucose detection, ACS Nano 6 (2012) 3206–3213.

[24] Y.X. Xu, K.X. Sheng, C. Li, G.Q. Shi, Self-assembled graphene hydrogel via a one-step hydrothermal process, ACS Nano 4 (2010) 4324–4330.

[25] M.A. Worsley, P.J. Pauzauskie, T.Y. Olson, J. Biener, J.H. Satcher, T.F. Baumann, Synthesis of graphene aerogel with high electrical conductivity, J. Am. Chem. Soc. 132 (2010) 14067–14069.

[26] K.W. Chen, L.B. Chen, Y.Q. Chen, H. Bai, L. Li, Three-dimensional porous graphene-based composite materials: electrochemical synthesis and application, J. Mater. Chem. 22 (2012) 20968–20976.

[27] C.G. Hu, H.H. Cheng, Y. Zhao, Y. Hu, Y. Liu, L.M. Dai, et al., Newly-designed complex ternary Pt/PdCu nanoboxes anchored on three-dimensional graphene framework for highly efficient ethanol oxidation, Adv. Mater. 24 (2012) 5493–5498.

[28] Z.S. Wu, S.B. Yang, Y. Sun, K. Parvez, X.L. Feng, K. Mullen, 3D nitrogen-doped graphene aerogel-supported Fe_3O_4 nanoparticles as efficient eletrocatalysts for the oxygen reduction reaction, J. Am. Chem. Soc. 134 (2012) 9082–9085.

[29] Z.P. Li, J.Q. Wang, S. Liu, X.H. Liu, S.R. Yang, Synthesis of hydrothermally reduced graphene/MnO_2 composites and their electrochemical properties as supercapacitors, J. Power Sources 196 (2011) 8160–8165.

[30] P. Si, X.C. Dong, P. Chen, D.H. Kim, A hierarchically structured composite of Mn_3O_4/3D graphene foam for flexible nonenzymatic biosensors, J. Mater. Chem. B 1 (2013) 110–115.

[31] W.S. Hummers, R.E. Offeman, Preparation of graphitic oxide, J. Am. Chem. Soc. 80 (1958) 1339.

[32] Y.X. Zhao, Z.Y. He, Z.F. Yan, Copper@carbon coaxial nanowires synthesized by hydrothermal carbonization process from electroplating wastewater and their use as an enzyme-free glucose sensor, Analyst 138 (2013) 559–568.

[33] J.J. Shi, J.J. Zhu, Sonoelectrochemical fabrication of Pd–graphene nanocomposite and its application in the determination of chlorophenols, Electrochim. Acta 56 (2011) 6008–6013.

[34] X.H. Kang, Z.B. Mai, X.Y. Zou, P.X. Cai, J.Y. Mo, A sensitive nonenzymatic glucose sensor in alkaline media with a copper nanocluster/multiwall carbon nano tube-modified glassy carbon electrode, Anal. Biochem. 363 (2007) 143–150.

[35] S.B. Yang, X.L. Feng, S. Ivanovici, K. Mullen, Fabrication of graphene-encapsulated oxide nanoparticles: towards high-performance anode materials for lithium storage, Angew. Chem. Int. Ed. 49 (2010) 8408–8411.

[36] X.M. Chen, G.H. Wu, J.M. Chen, X. Chen, Z.X. Xie, X.R. Wang, Synthesis of clean and well-dispersive Pd nanoparticles with excellent electrocatalytic property on graphene oxide, J. Am. Chem. Soc. 133 (2011) 3693–3695.

[37] A.P. Liu, T. Xu, Q.H. Ren, M. Yuan, W.J. Dong, W.H. Tang, Graphene modulated 2D assembly of plasmonic gold nanostructure on diamond-like carbon substrate for surface-enhanced Raman scattering, Electrochem. Commun. 25 (2012) 74–78.

[38] I. Platzman, R. Brener, H. Haick, R. Tannenbaum, Oxidation of polycrystalline copper thin films at ambient conditions, J. Phys. Chem. C 112 (2008) 1101–1108.

[39] F. Jiang, S. Wang, J.J. Lin, H.L. Jin, L.J. Zhang, S.M. Huang, et al., Aligned SWCNT–copper oxide array as a nonenzymatic electrochemical probe of glucose, Electrochem. Commun. 13 (2011) 363–365.

[40] S. Vadahanambi, J.H. Jung, I.K. Oh, Microwave syntheses of graphene and graphene decorated with metal nanoparticles, Carbon 49 (2011) 4449–4457.

[41] I. Nikov, K. Paev, Palladium on alumina catalyst for glucose-oxidation: reaction-kinetics and catalyst deactivation, Catal. Today 24 (1995) 41–47.

[42] I. Danaee, M. Jafarian, F. Forouzandeh, F. Gobal, M.G. Mahjani, Kinetic interpretation of a negative time constant impedance of glucose electrooxidation, J. Phys. Chem. B 112 (2008) 15933–15940.

[43] Q.Y. Wang, X.Q. Cui, J.L. Chen, X.L. Zheng, C. Liu, T.Y. Xue, et al., Well-dispersed palladium nanoparticles on graphene oxide as a non-enzymatic glucose sensor, RSC Adv. 2 (2012) 6245–6249.

[44] S.I. Mho, D.C. Johnson, Electrocatalytic response of carbohydrates at copper-alloy electrodes, J. Electroanal. Chem. 500 (2001) 524–532.

[45] C.L. Li, H.J. Wang, Y. Yamauchi, Electrochemical deposition of mesoporous Pt–Au alloy films in aqueous surfactant solutions: towards a highly sensitive amperometric glucose sensor, Chem. Eur. J. 19 (2013) 2242–2246.

[46] X.H. Niu, M.B. Lan, H.L. Zhao, C. Chen, Well-dispersed Pt cubes on porous Cu foam: high-performance catalysts for the electrochemical oxidation of glucose in neutral media, Chem. Eur. J. 19 (2013) 9534–9541.

[47] H.C. Gao, F. Xiao, C.B. Ching, H.W. Duan, One-step electrochemical synthesis of PtNi nanoparticle–graphene nanocomposites for nonenzymatic amperometric glucose detection, ACS Appl. Mater. Interfaces 3 (2011) 3049–3057.

[48] X. Cao, N. Wang, S. Jia, Y.H. Shao, Detection of glucose based on bimetallic PtCu nanochains modified electrodes, Anal. Chem. 85 (2013) 5040–5046.

[49] X.H. Niu, M.B. Lan, C. Chen, H.L. Zhao, Nonenzymatic electrochemical glucose sensor based on novel Pt–Pd nanoflakes, Talanta 99 (2012) 1062–1067.

[50] L. Meng, J. Jin, G.X. Yang, T.H. Lu, H. Zhang, C.X. Cai, Nonenzymatic electrochemical detection of glucose based on palladium-single-walled carbon nanotube hybrid nanostructures, Anal. Chem. 81 (2009) 7271–7280.

[51] C.X. Xu, Y.Q. Liu, F. Su, A.H. Liu, H.J. Qiu, Nanoporous PtAg and PtCu alloys with hollow ligaments for enhanced electrocatalysis and glucose biosensing, Biosens. Bioelectron. 27 (2011) 160–166.

[52] A.H. Liu, H.R. Geng, C.X. Xu, H.J. Qiu, A three-dimensional hierarchical nanoporous PdCu alloy for enhanced electrocatalysis and biosensing, Anal. Chim. Acta 703 (2011) 172–178.

[53] Y.Q. Dai, K.K. Shiu, Highly sensitive amperometric glucose biosensor based on glassy carbon electrode with copper/palladium coating, Electroanalysis 16 (2004) 1806–1813.

Biographies

Ming Yuan is a Master course student in the Zhejiang Sci-Tech University, China. His research interests are the synthesis and characteristic of nanosized materials.

Aiping Liu, Dr. degree, obtained from Harbin Institute of Technology, China in July 2008. Dr. Liu is employed by Center for Optoelectronics Materials and Devices in Zhejiang Sci-Tech University of China as an associate professor and a visiting researcher in State Key Lab of Silicon Materials in Zhejiang University of China. Current fields of interest of Dr. Liu are focused on metal-modified carbon-based nanomaterials and their application in electrochemical sensor or biosensor.

Ming Zhao is currently a candidate for Master degree in the Zhejiang Sci-Tech University, China. Her Master research focuses on nanocomposite carbon material and its application in sensor.

Wenjun Dong is a professor in the Zhejiang Sci-Tech University of China. His research includes biomaterials and their application in biosensors.

Tingyu Zhao is an associate professor in the Zhejiang Sci-Tech University of China. Her research includes nanomaterials and their application in optoelectronics devices.

Jiajun Wang is a professor in the Zhejiang Sci-Tech University of China. His research includes nanomaterials and their application in optoelectronics devices.

Weihua Tang is a professor in the Beijing University Posts and Telecommunications, China. His research includes thin films and coatings, and nanomaterials for optoelectronics devices and microfabrication technology.